Acta Cryst. (1998). A**54**, 338–347

Existence of Two Crystal Structures of the Complex α-D-Glucose · NaCl · H_2O (2:1:1) Verified by Three-Beam Diffraction Experiments

R. H. Mathiesen,[a] F. Mo,[a]* A. Eikenes,[a] T. Nyborg[a] and H. B. Larsen[b]

[a]*Institutt for fysikk, Norges Teknisk–Naturvitenskapelige Universitet, N-7034 Trondheim, Norway, and* [b]*Høgskolen i Stavanger, Post box 2557 Ullandhaug, Stavanger, Norway. E-mail: fmo@phys.ntnu.no*

(*Received 11 September 1997; accepted 8 December 1997*)

Abstract

Triplet phases from three-beam interference measurements have been used to resolve a case of apparent structural ambiguity. 13 crystals, all cut from one large single crystal of the complex α-D-glucose · NaCl · H_2O (2:1:1) were subjected to physical measurements of triplet phases, which involved studies of a set of *model-sensitive triplets* being particularly sensitive to the differences in structure between the two models. From 8 to 43 triplets were examined for each crystal specimen. The estimated phases have been compared with the corresponding quantities calculated for the refined structure models. A statistical analysis of the results provides highly significant evidence that both structure models are present, but do not coexist in the same crystal. One possible explanation for this apparent anomaly is that a phase transition may be induced by the mechanical stress applied during cutting of the hard and nearly perfect crystals. Triplet phases for structure verification and discrimination between similar structure models, as demonstrated in the present work, appears to be a novel and potentially powerful application of three-beam interference measurements.

1. Introduction

A crystal structure of the complex α-D-glucose · NaCl · H_2O (2:1:1) has been published by Ferguson *et al.* (1991). In this study, 3530 reflections with $I > 3\sigma(I)$, of a total 6274 reflections from merging 6814 observations, were used for the structure solution and refinement. The space group was determined as $P3_1$, with $a = b = 16.836(3)$ and $c = 17.013(4)$ Å. The complex was at the same time being studied also by another group. They found the same space group and closely similar cell parameters, but arrived at a structure (Fröhlich, 1989) that we have shown to be different. The data set used in the latter work comprised 8845 merged reflections, of which 8291 were employed with unit weights for the structure solution and refinement. In the following, we will refer to the two different structures and their associated sets of structure factors as CA for the quantities defining the Canadian structure model (Ferguson *et al.*, 1991) and GE for quantities corresponding to the German model (Fröhlich, 1989).

We have analyzed the two structures and described the real-space differences and similarities from least-squares refinements of the two against their original data sets (Mo *et al.*, 1997). The primary difference is an interchange of the Cl and water O positions, which is accompanied mainly by small translation adjustments of the glucose rings and a partial rearrangement of the H-bonding system. The structure changes imply significant differences in phase for about 50% of the structure factors. As a means to resolve this apparent contradiction, we intended to use physically estimated triplet phases. Estimates for triplet-phase invariants can be obtained from three-beam interference experiments (Post, 1977; Chang, 1982; Gong & Post, 1983; Thorkildsen & Mo, 1983; Mo *et al.*, 1988; Hümmer *et al.*, 1989; Weckert *et al.*, 1993). In the present case, the experimental work would involve measurement of selected triplet phases, of which the model-sensitive ones would be used to discriminate between the two models. A *model-sensitive three-phase invariant* contains at least one structure-factor phase that is significantly shifted by the difference in structure. By comparing our estimated triplet phases with those calculated for the refined models CA and GE, we expected to be able to identify one correct model of the pair.

2. Preliminary considerations

2.1. *The two phase sets*

The number of reflections employed for refinement differ substantially in the two data sets. We used 5054 reflections with $|F_o| > 10$ from the GE data set as the experimental basis for the generation of triplets, which implies that the number of structure factors is much larger than that actually used to refine the CA model.

There is a peculiar distribution of the single-phase differences, $|\Delta\varphi|$, between the two models. Phases for the largest $|F_o|$ are closely similar, thus for the 522 $|F_o| > 50$, the mean difference $\langle|\Delta\varphi|\rangle = 3.8°$. With an increasing number of weaker reflections, the $|\Delta\varphi|$ distribution becomes more bimodal. The result for all 5054 reflections in Fig. 1 shows very clearly the

bimodality, 96.2% of the $|\Delta\varphi|$ falling in one or other of the two ranges 0–30 or 150–180°. The average structure-factor amplitude $\langle|F_o|\rangle$ is 38.9 in the former range and 16.9 in the latter, respectively. The distribution of $|\Delta\varphi|$ for amplitudes with $|F_o| < 10$ is unimodally centered at ~165° with a uniform tail. In conclusion, it appeared very likely that a large number of measurable model-sensitive three-phase invariants could be generated from the 5054 reflections in the selected set.

From this basis, a total of 2.02×10^6 three-phase invariants were constructed. Among them, model-sensitive members with amplitudes suitable for phase measurements are extremely scarce. In the great majority of cases where model-sensitive single phases are involved, they occur in pairs, each with an intermodel $\Delta\varphi \sim \pm 180°$, thus rendering the model triplet-phase difference $\Delta\Phi_3 \sim 0°$. Only about 1100 of the invariants had $|\Delta\Phi_3| > 30°$ and in this group the best discriminators were combinations of one sensitive and two insensitive single phases. As it turned out, only about ten different sensitive single phases participate in multiple invariant combinations with insensitive pairs. Model-sensitive triplets with $30 < |\Delta\Phi_3| < 50°$ as a result of the accumulation of three individual small phase differences are much more abundant, but they were not employed extensively in the experiments due to their limited discriminatory ability.

In order to analyze the experimental results, we construct the variables

$$\Delta\Phi_3^{CA} = \Phi_3^{est} - \Phi_3^{CA} \quad (1)$$

$$\Delta\Phi_3^{GE} = \Phi_3^{est} - \Phi_3^{GE}, \quad (2)$$

where Φ_3^{est} is the triplet phase estimate assigned from the analysis of the three-beam interference intensity profiles, Φ_3^{CA} and Φ_3^{GE} are the corresponding values for the invariant calculated from the refined phases of model CA and model GE, respectively. If there are more than five independent estimates for each crystal,

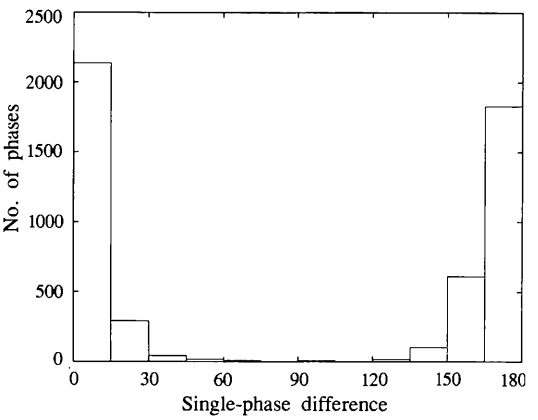

Fig. 1. Distribution of the single-phase differences between models CA and GE for 5054 reflections with $|F_o| > 10$.

the central limit theorem (Brandt, 1970) can be applied to adapt the n differences to the Gaussian distributions, $N(\mu, \sigma^2)$,

$$\sum_{j=1}^{n} \Delta\Phi_3^{CA} \sim N\left(\sum_{j=1}^{n} \mu_{CA}, \sum_{j=1}^{n} \sigma_{CA}^2\right) \quad (3)$$

$$\sum_{j=1}^{n} \Delta\Phi_3^{GE} \sim N\left(\sum_{j=1}^{n} \mu_{GE}, \sum_{j=1}^{n} \sigma_{GE}^2\right), \quad (4)$$

$\Delta\Phi_3^{CA}$ and $\Delta\Phi_3^{GE}$ have expected differences, μ_{CA}, μ_{GE} and variances σ_{CA}^2, σ_{GE}^2, respectively. The variances have two contributions:

$$\sigma_{CA,GE}^2 = \sigma_{est}^2 + \sigma_{ref\,CA,GE}^2, \quad (5)$$

where σ_{est}^2 is the variance associated with the estimate from the three-beam experiments and $\sigma_{ref\,CA,GE}^2$ is associated with the uncertainty in the phases calculated from the refined structures. The latter will not be quantified but serves to emphasize that the s.u.'s, $\sigma_{CA,GE}$, between the estimates and phases from a 'correct' model are expected to be larger than σ_{est}^2. If several three-phase invariants have multiple estimates from measurements on more than one crystal, σ_{est}^2 can be estimated as

$$S^2 = \left[\sum_{k=1}^{2}\sum_{j=1}^{t_k}(s_{j,k} - 1)\right]^{-1} \sum_{k=1}^{2}\sum_{j=1}^{t_k}\sum_{i=1}^{s_{j,k}}(\Phi_{3,i,j,k}^{est} - \langle\Phi_{3,j,k}^{est}\rangle)^2, \quad (6)$$

where

$$\langle\Phi_{3,j,k}^{est}\rangle = (1/s_{j,k})\sum_{i=1}^{s_{j,k}} \Phi_{3,i,j,k}^{est}.$$

In (6), k indicates the division of the estimates into two classes, $k = 1$ for CA crystals and $k = 2$ for GE crystals; t_k is the number of different triplets with more than one estimate for the crystals of class k,† $s_{j,k}$ is the number of different estimates for one particular triplet phase j of a specific class of crystals k. There will be $t_1 + t_2$ estimates of $\langle\Phi_3^{est}\rangle$ and therefore the same number of lost degrees of freedom for S^2.

The sample means of (3) and (4), $\hat{\mu}_{CA,GE} = \langle\mu_{CA,GE}\rangle = 0$ always. For a correct model, the mean differences are likely to be small; for an incorrect model, the individual differences will be randomly distributed in $[-\pi, \pi]$. The function

$$\hat{\sigma}_{CA,GE}^2 = (1/n)\sum_{j=1}^{n}(\Delta\Phi_3^{CA,GE})^2 \quad (7)$$

will be a sample of the total variance, $\sigma_{CA,GE}^2 + (1/n)\sum_{j=1}^{n}(\mu_{CA,GE} - \hat{\mu}_{CA,GE})^2$. The term in parentheses is a measure of the squared bias, *i.e.* a measure of the

† In this paper, the term 'A crystal of class ...' refers to the statistical concept of classification and must not be misinterpreted as a reference to the crystallographic classes.

difference between an estimated and a model phase that cannot be ascribed to random errors. In other words, if $\hat{\sigma}^2 \gg \sigma^2 \simeq S^2 + \sigma^2_{\rm ref} \geq S^2$, the estimates $\hat{\mu} = 0$ must be biased with respect to the true differences and the structure model is incorrect. A more sophisticated classification can be derived from confidence intervals for the statistical inference. From statistical calculus,

$$\hat{\sigma}^2_{\rm CA,GE}/\sigma^2_{\rm CA,GE} \sim \chi^2_n,$$

where n is the number of independent estimates and the degrees of freedom associated with the χ^2 observator. The statistical inference can be expressed as a $(1-\alpha)$ confidence interval for the standard uncertainty given that the mean estimates are unbiased:

$$\sigma_{\rm CA,GE} \in [(\hat{\sigma}^2_{\rm CA,GE}/Z_{1-\alpha/2,n})^{1/2}, (\hat{\sigma}^2_{\rm CA,GE}/Z_{\alpha/2,n})^{1/2}], \quad (8)$$

where $Z_{\alpha/2,n}$, $Z_{1-\alpha/2,n}$ are the lower and upper $\alpha/2$ quantiles of χ^2_n. If the mean estimate is unbiased, the lower boundary of the confidence interval (LBCI) should be similar to, or even smaller than, S. This will of course depend on the size of $\sigma^2_{\rm ref}$ but it is reasonable to expect $\sigma^2_{\rm ref} < \sigma^2_{\rm est}$. Accordingly, if LBCI $< S$, the experimental estimates fit the values calculated from the refined structure model. Model rejection can be performed at an α significance level from a Fisher test (F test) (Brandt, 1970). If $T = \hat{\sigma}^2_{\rm CA,GE}/S^2 > F_{\alpha,n,(s_1+s_2-t_1-t_2)}$, where T is the test observator and $F_{\alpha,n,m}$ is the α quantile of the F (Snedecor's F) distribution with n and m degrees of freedom, the structure model does not fit the experimental measurements and can be regarded as incorrect. In between these two situations, inference cannot be performed properly without a quantification of $\sigma^2_{\rm ref}$.

2.2. *The three-beam interference measurements*

In the standard procedure of the six-circle instrument (Hümmer *et al.*, 1987, 1989), a scan is made about the primary scattering vector **H** (Ψ scan), which is kept exactly in the Bragg-diffraction position in the horizontal plane. The detector monitors the primary diffracted intensity. During the rotation, a secondary reciprocal-lattice body L is carried through the Ewald sphere. The signed distance of L from the exact three-beam point, *the excitation error*, $\alpha_{\rm L}$, brings about a characteristic perturbation of $I_{\rm H}$, which will depend also on the structure-invariant triplet phase $\Phi_3 = \varphi_{-\rm H} + \varphi_{\rm L} + \varphi_{\rm H-L}$.

The three-beam perturbation of the kinematical intensity $I_{\rm H}$ has been expressed analytically for perfect finite crystals in the Laue–Laue case (Thorkildsen, 1987) from a solution of the Takagi–Taupin equations (Takagi, 1962, 1969; Taupin, 1964). A simplified functional form of the three-beam intensity, $I_{3,\rm H}$, serves to explain the terms that are most important for the phase estimation from intensity profiles

$$I_{3,\rm H}/I_{\rm H} \propto 1 - 2(c_1 l R_F)[(\cos\Phi_3) f_2(u) + (\sin\Phi_3) f_1(u)] + (c_1 l R_F)^2 [2 f_3(u) - (|F_{\rm H-L}|^{-2} + |F_{\rm L}|^{-2}) \times |F_{\rm H}|^2 f_1(u)]. \quad (9)$$

$I_{\rm H}$ is the kinematical intensity of the primary reflection, $c_1 = r_e \lambda V^{-1}_{\rm cell}$, where r_e is the classical electron radius, λ is the wavelength, $V_{\rm cell}$ is the volume of the unit cell and l is the typical crystal dimension. R_F is a ratio of structure-factor amplitudes

$$R_F = |F_{-\rm L}||F_{\rm L-H}|/|F_{\rm H}|. \quad (10)$$

$f_1(u) = (1/u^2)(1 - \cos u)$, $f_2(u) = (1/u)(1 - \sin u/u)$ and $f_3(u) = (1/u) f_2(u)$ are functions of a dimensionless excitation error, $u = 2\pi l \alpha_{\rm L}$, with $\alpha_{\rm L} = k_{\rm L} - K_{\rm 0}$; $k_{\rm L}$ and $K_{\rm 0}$ are the wavevector magnitudes of the secondary beam inside the crystal and the vacuum incident beam, respectively. Accordingly, $\alpha_{\rm L}$ and hence u are negative when L is inside the Ewald sphere and positive on the outside; $f_1(u)$ and $f_3(u)$ are non-negative and symmetrical about $u = 0$ where they have global maxima; $f_2(u)$ is antisymmetrical about $u = 0$, with $f_2(0) = 0$ and with signs as u itself.

To ease the interpretation, several quantities, such as beam path lengths, polarization terms and the effects from a divergent incident beam have been omitted in (9). A more complete treatment can be found in the work of Thorkildsen (1987). Plots of theoretical three-beam profiles are given both in this reference and by Weckert *et al.* (1993).†

The phase information resides in the middle term in (9). If $\Phi_3 \sim 0/\pi$, $f_2(u)$ will project out the phase-dependent perturbation as an asymmetry in the intensity profile near the exact three-beam point. This is the only asymmetric term in (9), thus asymmetry features in three-beam intensity profiles must relate to Φ_3. If $\Phi_3 \sim \pm\pi/2$, the perturbation will be symmetric with an extremum at $\alpha_{\rm L} = 0$ but the antisymmetry of the sine itself gives a maximum for $\Phi_3 = -\pi/2$ and a minimum for $\Phi_3 = \pi/2$. The profile for a general Φ_3 will contain a characteristic mixture of these extreme features, see for example Weckert *et al.* (1993).

The last term in (9) is a phase-independent perturbation. Experimentally, it is desirable to balance this term with respect to the phase term, to avoid suppression of the phase signal. This can be achieved by restricting the relative structure-factor amplitudes $|F_{\rm H}|$, $|F_{\rm L}|$ and $|F_{\rm H-L}|$ to lie within certain limits. If, for example, $|F_{\rm H-L}| \sim |F_{\rm L}| \gg |F_{\rm H}|$, energy will be transferred from reflection L into H *via* the coupling reflection $H - L$. This is the *Umweganregung* (Renninger, 1937). In (9), this situation corresponds to a large

† The two authors use opposite definitions for the triplet phase. Thorkildsen defines $\Phi_3 = \varphi_{\rm H} + \varphi_{-\rm L} + \varphi_{\rm L-H}$, Weckert *et al.* have $\Phi_3 = \varphi_{-\rm H} + \varphi_{\rm L} + \varphi_{\rm H-L}$. We follow here the definition of the latter authors.

R_F and consequently the last term ($\propto R_F^2$) will suppress the phase term ($\propto R_F$). The last term itself is roughly equal to $+2(c_1 l R_F)^2 f_3(u)$ since the amplitude contributions in front of $f_1(u)$ are small. Hence, the dominant intensity perturbation of I_H will be positive, phase independent and symmetrical about $\alpha_L = 0$. Conversely, if $|F_{H-L}| \sim |F_H| \gg |F_L|$, energy is transferred from H to L *via* $H - L$. This is the *Aufhellung* effect (Mayer, 1928). In this situation, $R_F \ll 1$ and a rough approximation leads to $-(c_1 l)^2 f_1(u)(|F_{H-L}|^2 + |F_L|^2)$ as the dominant perturbation to I_H. The resulting intensity profile will mainly display a phase-independent symmetrical minimum at $\alpha_L = 0$.

However, it is evident that *Umweganregung* and *Aufhellung* cases may exhibit asymmetry perturbations near the three-beam point that can only arise from the cosine phase term, whereas the sine phase term becomes negligible if the *Umweg* or *Aufhellung* effects are too dominant. A full investigation of the marginal phase effects in *Umweg* and *Aufhellung* cases must take into consideration the terms that have been eliminated from (9). In particular, the divergence of the incoming beam and divergence arising from crystal imperfections must be included.

Optimum experimental conditions for the physical estimation of three-phase invariants are obtained if R_F is restrained between certain boundaries. Weckert *et al.*, 1993) have recommended $2|F_H| \leq R_F < 6|F_H|$. Owing to the scarcity of model-sensitive triplets, we had to allow R_F values outside this range. Generally, this will lead to larger σ^2_{est}.

3. Experimental

The three-beam diffraction experiments were carried out on a six-circle Huber diffractometer (Hümmer *et al.*, 1987, 1989) at the time located on the Swiss–Norwegian Beamlines (SNBL), EH2. SNBL is supplied with radiation from the D1 bending magnet at the ESRF, Grenoble. An unfocused beam slitted down to about 0.8×0.8 mm was delivered at the sample position, located 16.7 m from a double-crystal Si(111) monochromator. The monochromator is located 30.8 m from the source. The unfocused beam divergencies in the sample position, including the contribution from the monochromator, are about 25 μrad horizontally and vertically at $\lambda = 1.0$ Å. The energy resolution of the monochromatic beam is $\Delta\lambda/\lambda \simeq 1.3 \times 10^{-4}$. The resolution in diffractometer angles was $1 \times 10^{-4\circ}$ in ω and Ψ and $2 \times 10^{-4\circ}$ in φ and χ.

A total of 13 different crystals were studied. Each crystal was cut from the same large single-crystal specimen and oriented from centering 12–15 reflections with $(\sin\theta/\lambda)_{max} = 0.4$ Å^{-1}. Cell parameters for the 13 crystals were equal within 1σ. For a crystal with a unit cell this size, *i.e.* $V_{cell} = 4180$ Å^3, there will be a large number of n-beam situations close to the one under study, and if strong reflections are involved they are likely to interfere with the measurement. The interference from other strong and closely adjacent reflections can be minimized by optimizing the wavelength for each triplet as described by Hümmer *et al.* (1990). In our experiments, the wavelength was optimized in one of the two ranges 0.9–1.2 or 1.0–1.35 Å by means of a computer program (Hümmer *et al.*, 1990).

The experimental work involves scanning the interference profiles of triplet pairs $-H/L/H - L$ and $H/-L/-H + L$, corresponding to phases $+\Phi_3$ and $-\Phi_3$, respectively. Two distinct right-handed cell matrices are possible in this space group, the (incorrect) alternative being (**b**, **a**, $-$**c**). It was ascertained that the choice of unit cell of the crystals was internally consistent and in agreement with the indexing of the native data sets CA and GE. A total of 309(×2) three-beam cases was studied. Owing to geometrical constraints which will depend on the particular orientation of a crystal on the diffractometer, a Ψ-scan of triplet $-H/L/H - L$ is taken to imply a scan of this triplet or any of its symmetry equivalents. Each intensity profile was scanned from 5 to 50 times depending on the scattering power of the primary reflection and the magnitude of the perturbation terms of (9). The suitable number of scans was determined in each case by visual verification of reliable counting statistics in all the details of the accumulated intensity profile. On average, data for a pair of three-beam profiles was collected in about 15 min of constant beam exposure. The Ψ-scan width was varied from ±0.04 to ±0.06° from the three-beam point with step size in the range 0.0002 to 0.0005°. The scan parameters were adjusted according to the increasing mosaicity of the crystals.

The measurements included 89 different triplets, of which 35 had an intermodel $|\Delta\Phi_3| < 30°$, hence, defined as *model insensitive*. A small subset of model-insensitive triplets was measured for about half of the crystals as a check on our experimental technique and the reproducibility of the phase assignments with crystals of different physical shapes and sizes. The remaining 54 triplets were selected from the group of 1100 model-sensitive invariants with $|\Delta\Phi_3| > 30°$, the latter group being dominated by a small number of frequently recurring sensitive single phases. The triplets chosen for measurements were generally good candidates regarding both model sensitivity and experimental requirements on the structure-factor amplitudes involved. For any crystal, some of the 54 triplets would be inaccessible due to physical constraints imposed by the particular orientation of the sample. The 54 triplets served adequately for the purpose of this work; in fact, none of the crystals lasted long enough in the X-ray beam to allow collection of all the model-sensitive profiles. The number of independent pairs of triplet-phase estimates ranged from 8 to 43 for the set of crystals employed.

The crystals of the complex (α-D-glucose)$_2$ · NaCl · H_2O are very hard and nearly perfect. Freshly cut specimens may have ω rocking curves with FWHM in the range 25–50 μrad. Exposure to X-rays initiates a chemical reaction that eventually induces several changes. The crystals do not deteriorate essentially during approximately the first 24 h of exposure,† after which period the mosaicity begins to increase. This process accelerates and when the FWHM has increased to about three times the initial value the crystals decay rapidly in another 1–2 h. With time and exposure, the crystals also change in appearance, from transparent and lustrous to opaque. Three-beam measurements were carried out on reflections with FWHM of ω rocking curves in the range 25–450 μrad.

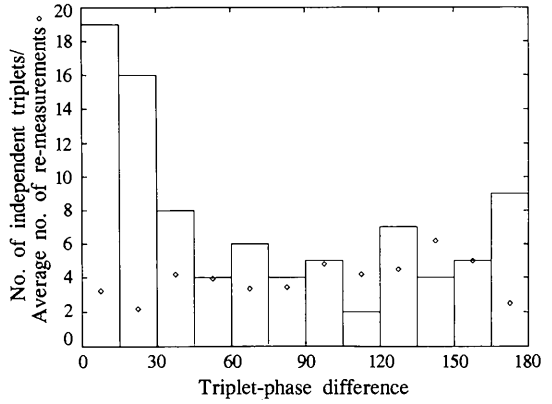

Fig. 2. Distribution of the intermodel triplet-phase differences from the measurements. The histogram shows the number of individual three-beam cases in each phase difference interval. The diamonds ◇ show the average number of measurements for each three-beam case in the intervals of the histogram.

4. Results

The distribution of triplet-phase differences between the two models for the three-beam cases studied are shown in Fig. 2. About 1/3 of the measurements were made on insensitive or slightly sensitive triplet phases. Some of these intensity profiles were checked as standards on several crystals and contribute to reduce the bias of the discarded model. However, some triplets, even with an intermodel difference of only 25–30°, can be sensitive if Φ_3^{GE} and Φ_3^{CA} are on either side of the characteristic values 0, $\pi/2$, π or $3\pi/2$. These are the points associated with sign inversions for the phase-dependent perturbation terms in (9). As was pointed out by Weckert *et al.* (1993), the experimental

† The time is given with reference to a storage ring fill current of 100 mA and wavelengths in the interval 0.9–1.35 Å.

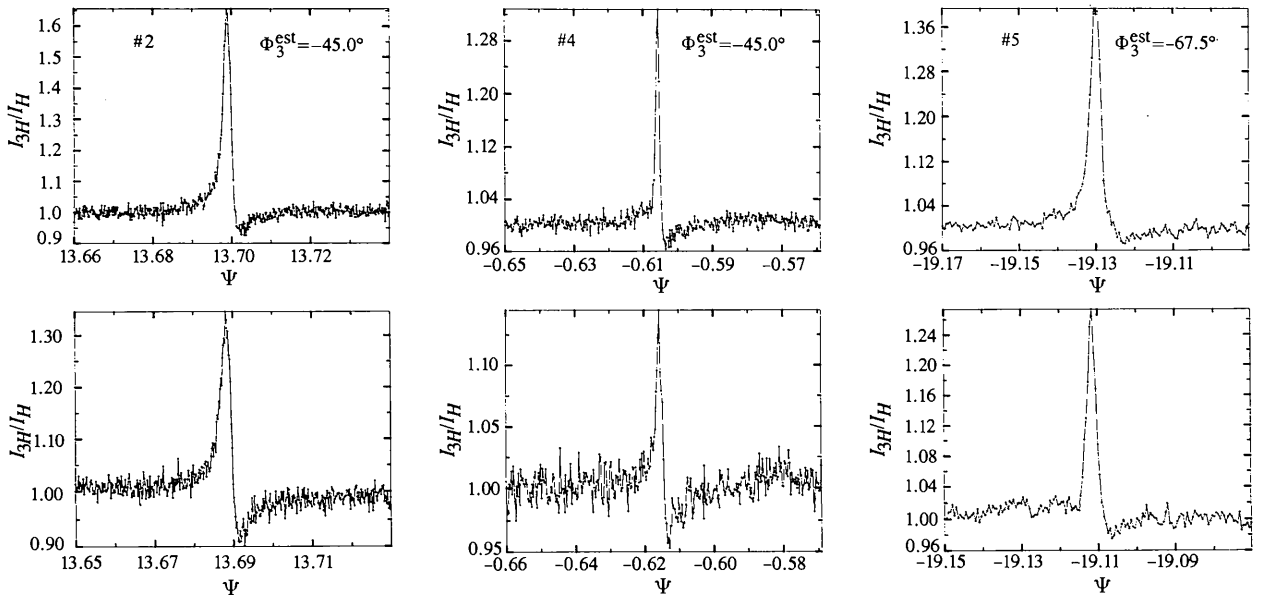

(*a*)

Fig. 3. Three-beam intensity profiles. The related pairs are stacked vertically with the estimated triplet phase, corresponding to triplet $-H/L/H-L$, and the crystal serial number given in the upper figure. (*a*) $30\bar{4}/2\bar{4}1/1\bar{1}45$, $|F_H| = 111.0$, $|F_L| = 266.6$, $|F_{H-L}| = 233.0$. $\Phi_3^{CA} = -48°$, $\Phi_3^{GE} = -65°$. (*b*) $2\bar{2}\bar{3}/14\bar{7}/1,\bar{2},10$, $|F_H| = 21.7$, $|F_L| = 103.0$, $|F_{H-L}| = 157.3$. $\Phi_3^{CA} = 105°$, $\Phi_3^{GE} = -66°$. (*c*) $2\bar{2}3/115/11\bar{2}$, $|F_H| = 21.7$, $|F_L| = 90.0$, $|F_{H-L}| = 161.5$. $\Phi_3^{CA} = -98°$, $\Phi_3^{GE} = 89°$. (*d*) $2\bar{2}5/\bar{6}35/8,\bar{1},\overline{10}$, $|F_H| = 20.2$, $|F_L| = 135.5$, $|F_{H-L}| = 98.1$. $\Phi_3^{CA} = -144°$, $\Phi_3^{GE} = -47°$. (*e*) $2\bar{2}\bar{3}/1,4,11/12\bar{8}$, $|F_H| = 21.7$, $|F_L| = 50.5$, $|F_{H-L}| = 161.5$. $\Phi_3^{CA} = -83°$, $\Phi_3^{GE} = 72°$. (*f*) $2\bar{2}3/5\bar{1}\bar{7}/\bar{3}34$, $|F_H| = 38.5$, $|F_L| = 172.9$, $|F_{H-L}| = 109.9$. $\Phi_3^{CA} = 19°$, $\Phi_3^{GE} = 69°$.

resolution for the phase estimation is improved near the characteristic values, especially for $\pi/2$ and $3\pi/2$, where the asymmetry of the intensity profile is reversed. Fig. 2 shows that the average number of measurements for the sensitive triplets is close to four. The low re-measurement frequency of the most sensitive triplets, *i.e.* in the interval 165–180°, is due to difficulties in locating good sampling positions adequately separated from neighboring multibeam situations.

A few of the 309 three-beam interference profile pairs are reproduced in Fig. 3 as examples of the experimental results. In the legend of each of the figures (*a*)–(*f*), the indices $-H/L/H-L$ of the three structure factors involved in this triplet are given along with the structure-factor amplitudes and the calculated triplet-phase values for the CA and the GE structures. For practical purposes, the structure factors are $|F_o|$'s from the GE data. The crystal serial No. and the estimated triplet phase are given in the upper figure corresponding to the $-H/L/H-L$ triplet of the pair.

In Fig. 3(*a*), three intensity profiles of the same model-insensitive triplet pair are shown. Crystal No. 2 was later classified as CA, No. 4 and No. 5 as GE. All these profiles have a depression for $\Delta\Psi > 0\,(\alpha_L > 0)$

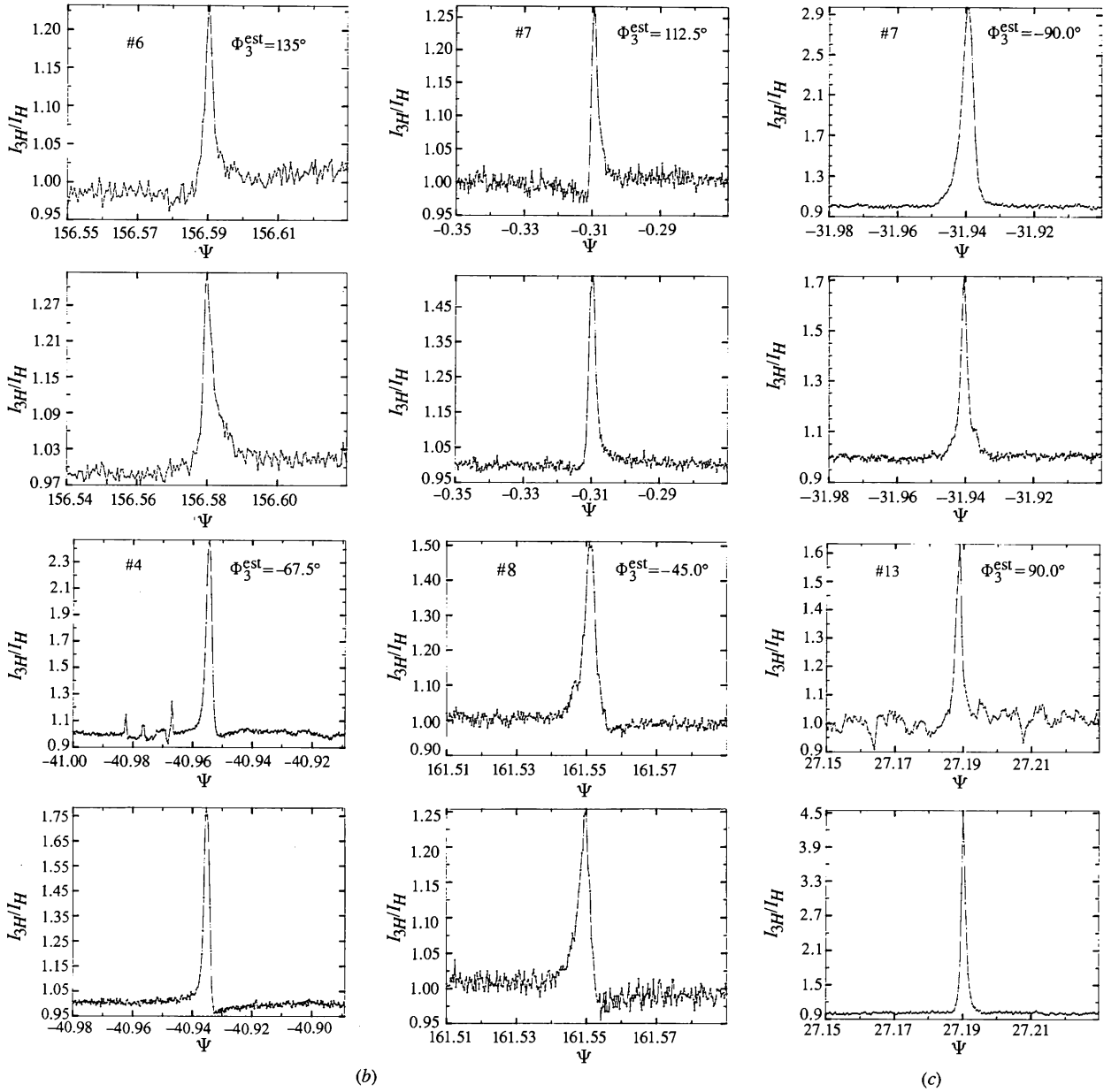

Fig. 3 (*cont.*)

near the three-beam point, $\Delta\Psi = 0$, characteristic for a 0-type Φ_3, and the magnitude of the interference peak is in all cases larger for the upper member of a triplet pair, which identifies the fourth quadrant as the proper one. A more detailed study of the relative magnitudes of these effects led to the phase assignments given in the figures. Fig. 3(*b*) shows a model-sensitive case with $|\Phi_3^{CA} - \Phi_3^{GE}| \sim 170°$ measured on four different crystals. Crystals 6 and 7 were later assigned to the CA class, Nos. 4 and 8 both to GE. A conspicuous feature in these profiles is the reversal of asymmetry between the two classes of crystals, Nos. 6 and 7 show π-type asymmetry, Nos. 4 and 8 have Φ_3 closer to 0. Also, the relative magnitudes of the interference maxima are reversed between the two classes but are, like the asymmetry, consistent for specimens of the same class. A rough assignment immediately places Φ_3 for the triplet $-H/L/H-L$ of class CA in the second quadrant and that of class GE in the fourth quadrant. More quantitative assessments of the interference effects led to the estimated phases shown in the figures. Fig. 3(*c*) displays two profile pairs for another three-beam case with $|\Phi_3^{CA} - \Phi_3^{GE}| \sim 170°$, crystal 7 is CA, 13 is GE. This is a case where the phase-independent

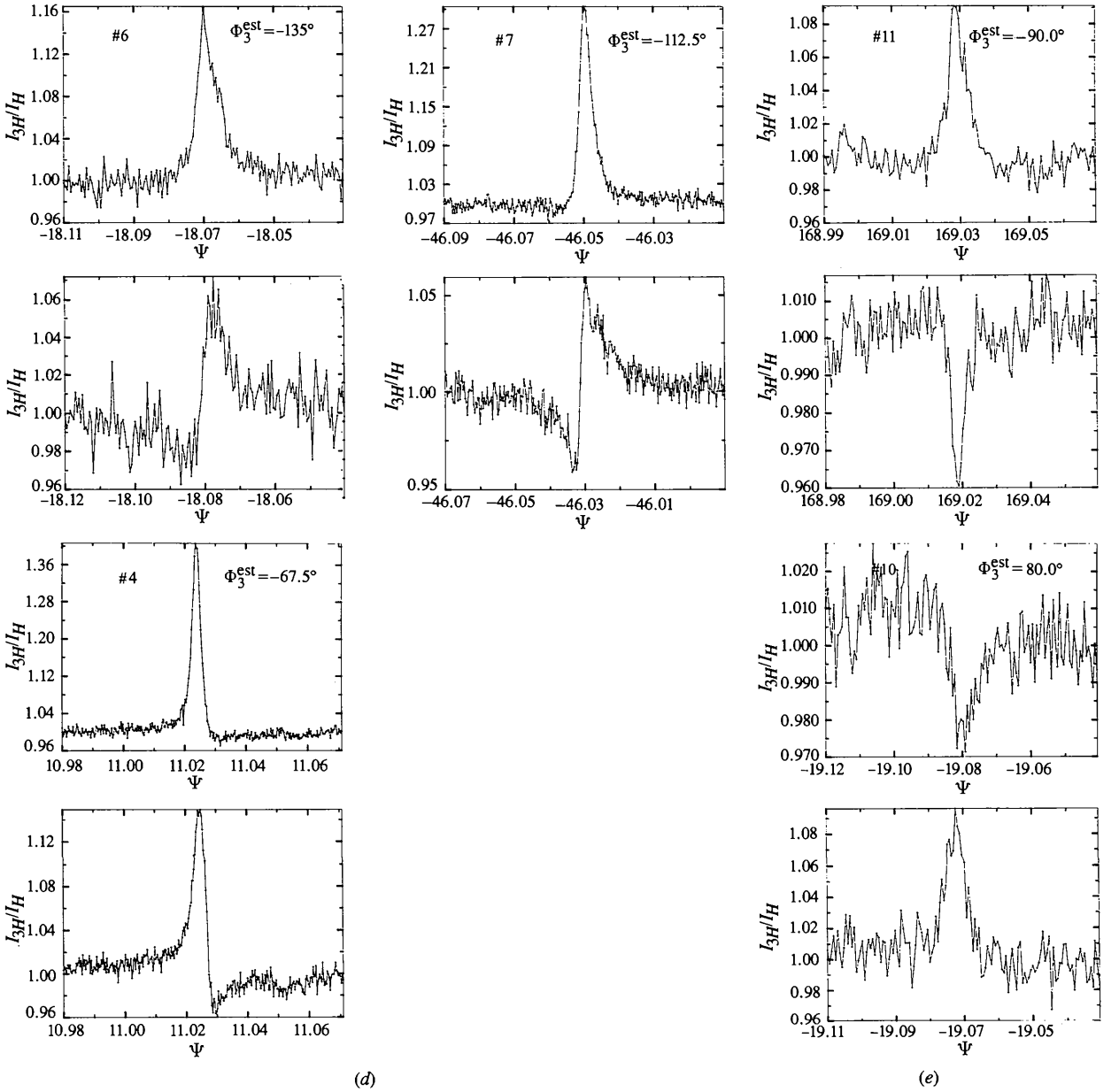

Fig. 3 (*cont.*)

Umweganregung is quite strong. The model phases predict a phase-dependent perturbation predominantly from the sine term in (9). In spite of the strong *Umweg* contribution, good estimates of the triplet phases could be made. A case of intermediate sensitivity with an intermodel $|\Delta\Phi_3| \sim 100°$ is shown in Fig. 3(*d*). Crystals 6 and 7 are CA, 4 is GE. While the relative amplitude sequence is the same for all pairs, the reversal of asymmetry makes discrimination between the two types facile. Fig. 3(*e*) illustrates a case for which the kinematical scattering of the primary reflection is weak and *Umweg* effects are small since the scattering power of the secondary reflection L is intermediate. These profiles were scanned many times to obtain sufficient counting statistics. The triplet phase for crystal 11 was estimated at $-90°$, a very weak 0-type asymmetry in the parent triplet profile for crystal 10 is the reason for assigning $\Phi_3^{est} = 80°$. Finally, four profile pairs for a three-beam case with a $|\Delta\Phi_3| \sim 50°$ are shown in Fig. 3(*f*). Crystals 6 and 7 are CA, 4 and 10 are GE. Here the discriminatory power is limited not only by the modest model difference but also by the fact that the two triplet phases belong to the same phase quadrant. Nevertheless, the difference in magnitude between the

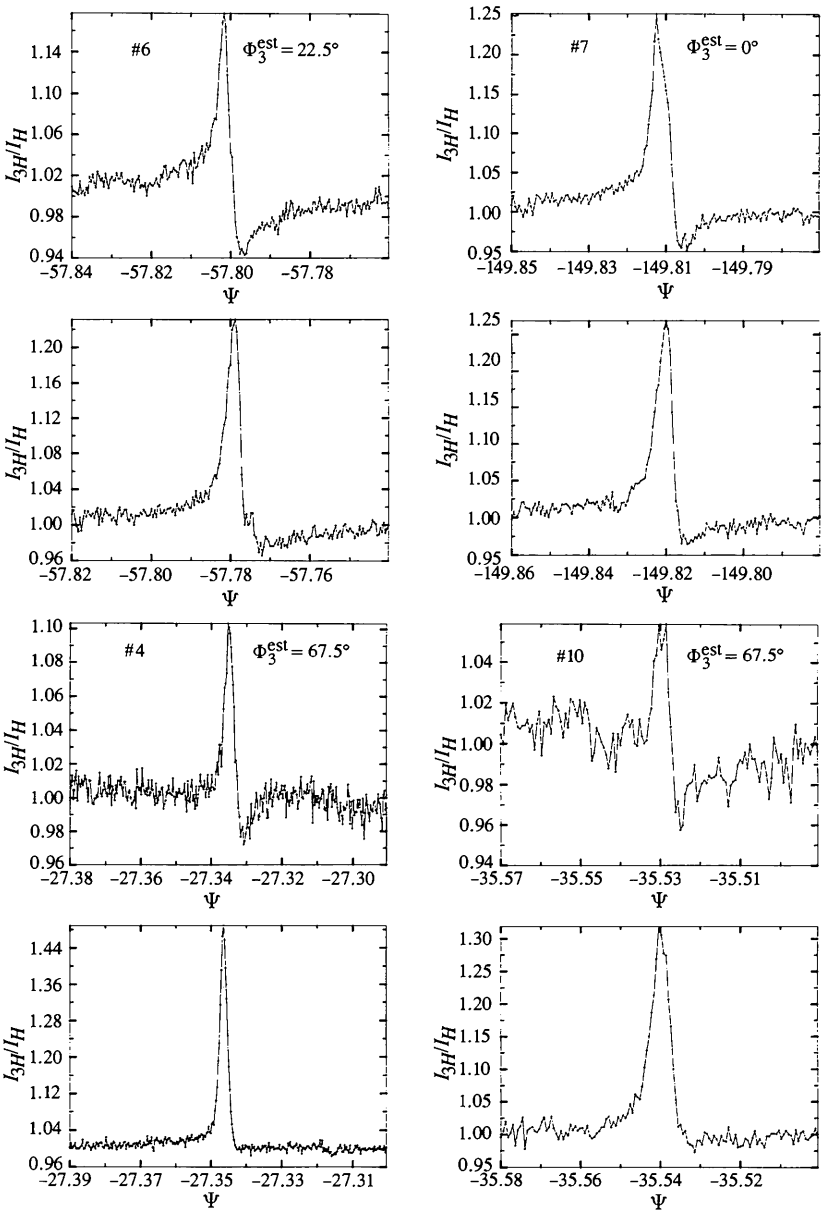

(*f*)

Fig. 3 (*cont.*)

two triplet phases are reproduced semiquantitatively by the measurements. Note that profiles of different three-beam cases leading to the same estimate for the phase may appear quite dissimilar as a result of different phase-independent contributions which are related in particular to the relative magnitudes of the three structure factors, the beam path lengths in the crystal and polarization effects. It is imperative, therefore, that pairs of profiles, $-H/L/H-L$ and $H/-L/-H+L$, collected from the same crystal, are compared directly to extract the phase-dependent information.

All the estimated triplets, including the model-insensitive ones, have been employed in the phase statistics. In principle, the crystals could have been distinguished qualitatively from the Ψ scans of only one Friedel-related pair of highly sensitive triplets. For a more quantitative comparison of the two models, this strategy is inadequate, however. Several model-sensitive phases are required to probe in detail the (postulated) differences in structure. In a statistical sense, several estimated triplet phases are needed to discard one of the models with a reliable significance from a test statistic. Including the model-insensitive triplets will increase the number of degrees of freedom for the test statistic, but will as well reduce the bias for the discarded model. The contribution to the test statistic from the model-insensitive triplets is therefore of less importance. Following (6), the inference for estimating σ^2_{est} is given in Table 1. The estimated variance associated with the experimental phase estimates is $(19.7°)^2$. Weckert *et al.* (1993) reported $(17°)^2$ for their triplet-phase estimates of tetragonal lysozyme relative to the values calculated from the structure model.†

In Table 2, $\hat{\sigma}$ for the 13 crystals are presented together with 99% confidence intervals for σ. From these results, it is evident that at least two distinct crystal structures must exist. The classification gives seven crystals in agreement with the GE model and six crystals that fit the CA model. Further analysis of the total variances shows that for every crystal, except No. 12, one of the two confidence intervals has a LBCI $< S$. For all crystals, the model with the largest $\hat{\sigma}$ can be rejected at a significance level $\alpha \ll 0.001$ for the F-test observator T. The mean total variances, $\hat{\sigma}^2$, for the 'correct' models are somewhat larger than the random errors, S^2, but not more than expected considering the uncertainty in the phases of the refined models, in particular since weak and intermediate structure-factor amplitudes comprise a large fraction of the reflection basis. Crystal 3 is a special case since we for this crystal accidentally made about 50% of the measurements with the incorrect right-handed matrix (**b**, **a**, −**c**) and thereby sampled random three-beam cases, all of them with

† This estimate was based on a mixture of general and special phase values. Our estimate is based on general phases.

Table 1. *The random errors of the experimental phase estimation procedure*

Crystal classification, k	CA ($k=1$)	GE ($k=2$)
Different multiple estimates, t_k	$t_1 = 52$	$t_2 = 38$
No. of multiple estimates, $\sum s_{j,k}$	$\sum s_{j,1} = 145$	$\sum s_{j,2} = 112$
Class variance	$S_1^2 = (19.0°)^2$	$S_2^2 = (20.5°)^2$
Total variance	$S^2 = (19.7°)^2$	

model-insensitive triplet phases. In Table 2, this is seen as a low $\hat{\sigma}$ for the discarded model since this model also fits the large fraction of insensitive triplets. The intervals of crystal 12 are biased due to two outliers, nevertheless the intervals do discriminate well in favor of a GE classification. For the discarded models, it is clear that the differences cannot be explained by $S^2 + \sigma^2_{\text{ref}}$ alone. Consequently, there must be a bias between experimental estimates and the structure model calculations.

Some of the three-beam cases under study involved rather large *Umweg* or *Aufhellung* effects. In fact, most of the sensitive triplets were outside the recommended range of R_F. A closer investigation reveals that successful estimates have been carried out on triplets predominantly in the region $|F_{\mathbf{H}}| \le R_F < 100|F_{\mathbf{H}}|$, but we have also estimated a few phases from profiles with R_F up to $240|F_{\mathbf{H}}|$. For the triplets with the largest R_F's, the reliability of the sine assignment for the triplet phase is consistently poor.

5. Conclusions

In this work, we have demonstrated that triplet phases estimated from three-beam interference measurements can be used to study a case of apparent structural dimorphism. Measurements on 13 different single-crystal specimens cut from the same large crystal of the complex (α-D-glucose)$_2$ · NaCl · H_2O show unambiguously that there exist two distinct crystal structures and the set of crystals can be assigned with high statistical significance to belong to either one or the other. As the preparation of small crystal pieces used for these experiments rules out the possibility that they are distinct domains of the larger crystal, we are led to propose that this is a case of a phase transition, presumably induced by the mechanical stress applied during cutting. We note in this context that some of the cut specimens became strongly static.

Could the two crystal structures have been distinguished reliably based on measured intensities alone? The standard R_{merge} calculated for 6065 identical and properly scaled $|F_o|^2$ from the two data sets was 0.095. The discrepancies between the two data sets are found among the weak reflections. Taking this into account and considering that the individual refinements of the

Table 2. *99% confidence intervals for $\sigma_{CA,GE}$ of the 13 crystals of $(\alpha$-D-Glc$)_2 \cdot NaCl \cdot H_2O$*

Intervals with the upper boundary 180° have a confidence level <99%. However, all 95% confidence intervals have an upper limit <180°.

Crystal No.	n	$\hat{\sigma}_{CA}$ (°)	$\hat{\sigma}_{GE}$ (°)	99% σ_{CA} interval (°)	99% σ_{GE} interval (°)	Classification
1	11	97.6	23.7	[62.6, 180]	[15.2, 48.7]	GE
2	28	25.7	100.6	[19.1, 38.5]	[74.5, 150.8]	CA
3	29	24.6	76.3	[18.3, 36.6]	[56.8, 113.4]	CA
4	34	95.5	23.3	[72.6, 136.4]	[17.7, 33.3]	GE
5	8	83.6	10.5	[50.5, 180.0]	[6.3, 25.6]	GE
6	33	22.4	85.2	[17.0, 32.3]	[64.4, 122.8]	CA
7	43	19.7	77.0	[15.4, 27.0]	[60.1, 105.6]	CA
8	17	109.4	20.7	[75.4, 180]	[14.3, 35.7]	GE
9	15	25.7	72.9	[17.4, 46.4]	[49.3, 131.6]	CA
10	20	120.7	19.7	[85.4, 180]	[13.9, 32.3]	GE
11	29	23.2	113.0	[17.2, 34.4]	[84.1, 168.0]	CA
12	29	99.1	29.7	[73.7, 147.3]	[22.1, 44.2]	GE
13	13	115.1	19.0	[76.0, 180]	[12.6, 36.3]	GE

two models against their native data sets gave R based on $|F_o|^2$ in the range 0.06–0.07, it is not obvious that the differences in structure would have been revealed from standard crystallographic studies based on structure-factor amplitudes. What can be stated clearly is that the latter approach would require high-quality data collected from two different crystals, one of each model. In comparison, collecting three-beam interference profiles for a few model-sensitive triplets, if feasible, is far more efficient and has much greater discriminatory potential.

A detailed study of the differences in the two structures is under way (Mo *et al.*, 1997). An investigation of changes in macroscopic physical properties possibly induced by mechanical stress is also needed.

We are greatly indebted to Dr Edgar Weckert, Kerstin Hölzer and Klaus Schröer of the University of Karlsruhe for much help and expert advice in the use of the six-circle Huber diffractometer and the programs for instrument control and data acquisition. We are grateful to the ESRF for generous allotments of beam time (Projects MI-117 and HS-37), as well as to SNBL (Projects 01-02-02, 01-02-07 and 01-02-46). Thanks are due to Dr R. Fröhlich, University of Münster, for providing large crystals of the complex, and to Norges Forskningsråd (NFR) for Grant 101166/431 in support of this work.

References

Brandt, S. (1970). *Statistical and Computational Methods in Data Analysis*, pp. 78–79, 382. Amsterdam: North-Holland.
Chang, S.-L. (1982). *Phys. Rev. Lett.* **48**, 163–166.
Ferguson, G., Kaitner, B., Connett, B. E. & Rendle, D. F. (1991). *Acta Cryst.* B**47**, 479–484.
Fröhlich, R. (1989). Personal communications.
Gong, P. P. & Post, B. (1983). *Acta Cryst.* A**39**, 719–724.
Hümmer, K., Bondza, H. & Weckert, E. (1987). *Acta Cryst.* A**43**, C222.
Hümmer, K., Weckert, E. & Bondza, H. (1989). *Acta Cryst.* A**45**, 182–187.
Hümmer, K., Weckert, E. & Bondza, H. (1990). *Acta Cryst.* A**46**, 393–402.
Mayer, G. (1928). *Z. Kristallogr.* **66**, 585–636.
Mo, F., Hauback, B. C. & Thorkildsen, G. (1988). *Acta Chem. Scand. Ser. A*, **42**, 130–138.
Mo, F., Mathiesen, R. H. & Eikenes, A. (1997). In preparation.
Post, B. (1977). *Phys. Rev. Lett.* **39**, 760–763.
Renninger, M. (1937). *Z. Phys.* **106**, 141–176.
Takagi, S. (1962). *Acta Cryst.* **15**, 1311–1312.
Takagi, S. (1969). *J. Phys. Soc. Jpn*, **26**, 1239–1253.
Taupin, D. (1964). *Bull. Soc. Fr. Minéral. Cristallogr.* **87**, 469–511.
Thorkildsen, G. (1987). *Acta Cryst.* A**43**, 361–369.
Thorkildsen, G. & Mo, F. (1983). Eighth European Crystallographic Meeting (ECM-8), Liège, Belgium. Abstracts, p.258.
Weckert, E., Schwegle, W. & Hümmer, K. (1993). *Proc. R. Soc. London Ser. A*, **442**, 33–46.